JCTC Journal of Chemical Theory and Computation

Article

pubs.acs.org/JCTC

Analysis of the Rotational−Vibrational States of the Molecular Ion H_3^+

Tibor Furtenbacher,[†,‡] Tamás Szidarovszky,[†,‡] Edit Mátyus,[†] Csaba Fábri,[†] and Attila G. Császár*[,†,‡]

[†]Laboratory of Molecular Structure and Dynamics, Institute of Chemistry, Eötvös University, H-1117 Budapest, Pázmány Péter sétány 1/A, Hungary

[‡]MTA-ELTE Research Group on Complex Chemical Systems, H-1518 Budapest 112, P.O. Box 32, Hungary

Supporting Information

ABSTRACT: On the basis of both experiment and theory, accurate rotational−vibrational line positions and energy levels, with associated critically reviewed labels and uncertainties, are reported for the ground electronic state of the H_3^+ molecular ion. An improved MARVEL algorithm is used to determine the validated experimental levels and their self-consistent uncertainties from a set of 1610 measured transitions and associated uncertainties, coming from 26 sources. 1410 transitions have been validated for *ortho*-H_3^+ and *para*-H_3^+, 78 belong to floating components of the spectroscopic network (SN) investigated and thus left unvalidated, while 122 measured transitions had to be excluded from the MARVEL analysis for one reason or another. The spectral range covered by the experiments is 7−16 506 cm^{-1} . Altogether 13 vibrational band origins are reported, the highest J value, where J stands for the rotational quantum number, for which energy levels are validated is 12. The MARVEL energy levels are checked against ones determined from accurate variational nuclear motion computations employing the best available adiabatic ab initio potential energy surface and exact kinetic energy operators. The number of validated and thus recommended experimental-quality rovibrational energy levels is 652, of which 259 belong to *ortho*-H_3^+ and 393 to *para*-H_3^+. There are 105 further energy levels within floating components of the SN. The variational computations have been performed both without and with a simple nonadiabatic correction, whereby nonadiabaticity is modeled by the use of a non-nuclear vibrational mass. The lists of validated lines and levels for H_3^+ are deposited in the Supporting Information to this paper.

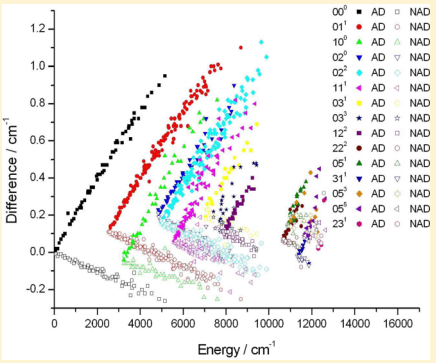

1. INTRODUCTION

The highly stable protonated H_2 molecule, the H_3^+ molecular ion, is the simplest polyatomic molecule. While it is unusual under terrestrial conditions, it is of considerable practical importance in outer space.[1−4] Part of its importance comes from the fact that its formation reaction, $H_2^+ + H_2 \rightarrow H_3^+ + H$, is strongly exothermic. The H_3^+ ion drives the chemistry in many cold parts of the universe, where only barrierless ion−molecule reactions ($H_3^+ + X \rightarrow HX^+ + H_2$) are feasible.[5,6] The H_3^+ ion is also an important tracer of the chemistry of the interstellar medium.[7] For these reasons and others, it is important to know as much as possible about the energy level structure of H_3^+ as well as about its nuclear dynamics and spectra, below and above the first dissociation asymptote, in various and extremely different environments. The H_3^+ ion has also been playing a very special role in the development of the quantum theory of nuclear motions and the understanding of the complex rotational−vibrational spectra of polyatomic molecules.[8] In particular, it has become the number one polyatomic molecule to study the effects of nonadiabaticity on high-resolution and high-excitation molecular spectra.[9−11] For this one also needs accurate experimental energy levels which one can use as reference values when comparing theory to experiment.

The electronic structure of the H_3^+ ion is as simple as one can expect for a closed-shell two-electron system, the ground electronic state is relatively well separated from all the excited electronic states.[12−14] The equilibrium structure of the ground electronic state of H_3^+ is an equilateral triangle, corresponding to D_{3h} point-group symmetry. Of the three fundamental vibrations of H_3^+ one can be characterized as an infrared inactive stretching (symmetric "breathing") vibration, ν_1, while the other one is an infrared active degenerate bending mode, ν_2. The fundamental $\nu_2 \leftarrow 0$ is by far the strongest spectral signature of H_3^+ and thus the corresponding spectral region was studied first in the laboratory.[15] Due to the low absorption intensities it is hard to observe the rotational−vibrational spectra of the ion, which led to the development of special experimental techniques for the detection of the transitions.[13] The H_3^+ ion rotates as an oblate symmetric top and has very small moments of inertia. For H_3^+, the rotational constants B and C are about 44 and 21 cm^{-1}, respectively.[16]

The nuclear dynamics of the H_3^+ ion exhibits several unusual features. Due to the lightness of the H atoms, the vibrations of H_3^+ are of very large amplitude, separation of the vibrational

Received: May 27, 2013
Published: November 5, 2013

Table 1. Experimental Data Sources for H_3^+ [a]

tag	range (cm^{-1})	trans (A/V)	vibrational band, v_1 v_2 L_2	J_{max}
04OkEp[44]	7.255−1695.9	100/98	$(00^0),01^1,02^2$	10
87MaMaMcJo[27]	1798.4−3212.4	113/109	01^1	10
94MaMcSaWa[37,b]	1843.5−4948.6	241/199	$01^1,02^2,02^0,11^1,03^3,03^1,12^2,10^0,12^0$	14
97DiNePoTe[64,c]	1881.8−3293.8	118/84	$03^3,11^1$	7
90BaReOk[30,d]	2089.3−2944.8	119/119	$11^1,02^2,02^0,01^1$	9
84WaFoMcBe[26]	2217.4−3029.8	51/50	$(00^0),01^1$	7
92XuRoGaOk[34,e]	2418.9−3290.8	73/65	$01^1,11^1,10^0,02^2$	13
01LiMc[16,f]	2436.6−3002.7	45/42	$11^1,03^3$	10
90NaItSuTa[29]	2457.2−2762.1	12/11	01^1	3
80Oka[15]	2457.2−2918.0	15/14	01^1	4
81Oka[24]	2457.2−3029.8	30/27	01^1	7
13WuLiLiLi[49]	2518.2−2918.0	12/12	01^1	4
94UyGaJaOk[36]	2691.4−3579.3	75/61	$01^1,10^0$	16
12CrHoSiPe[48]	2725.9−2725.9	1/1	01^1	2
01LiRaOk[42,g]	2860.5−3596.2	258/217	$01^1,02^2,03^1,11^1,03^3,02^0,12^2,10^0,20^0$	16
89MaFeWaMi[28]	4539.7−5094.2	50/43	02^2	12
90XuGaOk[31]	4557.0−5094.2	34/34	02^2	10
94VeCaGuJo[35]	6806.6−7265.9	15/14	03^1	5
91LeVeCaOk[32]	6865.7−6891.8	4/3	03^1	5
04MiKrWePl[45]	7192.8−7241.2	3/3	03^1	3
00McOk[40]	7785.2−8163.1	30/29	$12^2,21^1$	6
09MoGoOk[25]	10322−13676	143/109	$22^2,04^4,05^1,05^3,31^1,22^0,05^5,14^0,14^2,14^4,23^1$	7
08VeLeAgBe[65]	10726−13056	12/12	$22^2,05^1,05^3,06^2,14^2,14^4$	4
12 PaAdAlZo[13]	10752−16506	10/10	$22^2,05^1,07^1,08^2,16^2,16^4,25^1,34^2$	2
03GoMcOk[43]	11019−12419	22/21	$22^2,05^1,31^1,05^5,23^1,14^2,14^4$	4
08KrBiRePe[47]	11228−13332	23/23	$05^1,31^1,05^5,14^0,14^2,23^1,06^2,14^4,23^3,32^2$	2

[a]The tags listed are used to identify experimental data sources throughout this paper. The range given represents the range corresponding to wavenumber entries within the MARVEL input file and not to the range covered by the relevant experiment. Original and improved uncertainties of the individual lines can be obtained from the Supporting Information. Trans = transitions; A = no. of transitions available in the given source; V = no. of transitions validated for the given source. J_{max} = maximum J value of the observed transitions. This can be higher than the highest validated J as some of these transitions form part of floating components and thus cannot be validated via MARVEL. (00^0) means that combination difference (CD) relations, 69 and 6 based on 04OkEp[44] and 84WaFoMcBe,[26] respectively, were used as input data to MARVEL. [b]Table 1 of this source contains newly measured transitions as well as labeled transitions from 90XuGaOk.[31] Consequently, transitions reported in 90XuGaOk[31] are not included in the MARVEL analysis explicitly. We used the relabeled transitions published in Table 2 of 97DiNePoTe, except for the 3003.250 cm^{-1} transition, where we used the original label. [c]Contains 118 newly assigned transitions published first in 90BaReOk[30] and 92XuRoGaOk.[34] [d]Contains 136 unassigned transitions. [e]Contains 89 unassigned transitions. We used the relabeled transitions published in Table 2 of 97DiNePoTe,[64] except for the 3005.898 and 3249.699 cm^{-1} transitions, where the original labels were retained. [f]Contains two floating components, explaining why two measured transitions are not validated. [g]28 transitions are part of floating components.

and rotational degrees of freedom is poor, adiabatic and nonadiabatic effects become overly important,[11,17] and the usual perturbational treatments and effective Hamiltonians used for interpreting molecular spectra have poor convergence characteristics. Thus, only variational techniques are applicable for the interpretation of the complex rotational−vibrational spectra of the ion. Sophisticated variational nuclear motion techniques, limited in accuracy principally by the accuracy of the potential energy surface (PES) employed and nonadiabatic effects, have indeed been developed to treat all bound rovibrational states and also resonance states beyond the first dissociation asymptote.[10,11,18−23]

Initiated mainly by work in the Oka group,[15,24] high-resolution spectra of H_3^+ have been the subject of a number of experimental investigations resulting in a relatively large quantity of moderately accurate data[13,15,16,24−48] and a small set of highly accurate transitions.[49] The last comprehensive, critical evaluation of the measured data for H_3^+ was performed in 2001 by Lindsay and McCall.[16] They obtained 526 rovibrational energy levels below 9886 cm^{-1}. In the present study, based on experimental results also used by Lindsay and McCall[16] but augmented with several more recent measurements, we perform a systematic analysis of the measured rovibrational spectra corresponding to the ground electronic state of H_3^+. This is done via the latest implementation[50] of the MARVEL protocol,[50−53] where the abbreviation stands for measured active rotational−vibrational energy levels. MARVEL can invert, in a weighted least-squares sense, the measured transition data and results in accurate, experimental-quality energy levels with dependable, self-consistent (within the limits of the experimental measurements considered) uncertainties. The method has been employed successfully to determine the rovibrational states of several water isotopologues[54−56] and of parent ketene.[57] It has also been employed recently[58] to treat the measured transitions of the H_2D^+ and D_2H^+ isotopologues of H_3^+ and determine the corresponding rovibrational energy levels. Thus, the present study can be considered as a significant extension of the work started in ref 58, as well as that of Lindsay and McCall.[16] The present study goes much beyond 9886 cm^{-1}, the energy limit in the study of Lindsay and McCall,[16] up to 16 506 cm^{-1}.

A distinguishing feature of the present study is that we apply the theory of spectroscopic networks (SN)[59,60] and consider *all* measured and assigned transitions, while in ref 16 only the

"best" transitions were employed. We believe it is better to consider all transitions with proper uncertainties when determining "experimental" energy levels. Another important feature of this study is the utilization of all available experimental and the best first-principles transition and energy level data on an equal footing. For this purpose, we executed extensive variational rovibrational computations employing the best available adiabatic potential energy surface (PES) of H_3^+, called GLH3P,[13,14] whose intrinsic accuracy in the energy region considered is only a few 0.01 cm^{-1} and exact kinetic energy operators expressed in internal coordinates. Note also that a (partial) linelist for H_3^+ has been prepared by Tennyson and co-workers.[61] MARVEL-type efforts help to replace as many computed lines with their experimental counterparts as possible, paving the way to an understanding of the complete spectrum of H_3^+ below and beyond the first dissociation asymptote. Finally, we note that an extreme amount of H_3^+ lines have been detected by Carrington et al.[62,63] close to dissociation. Since these lines have been left unassigned for over 30 years, they cannot be used in the present MARVEL analysis. Nevertheless, it is hoped that results of the present study will help in the future understanding of the near-dissociation features of H_3^+ spectra.

2. MARVEL METHODOLOGY

MARVEL simultaneously processes all the available labeled experimental lines and the associated energy levels. While the energy levels could be called experimental or empirical, in order to emphasize the process they were derived from in this study, the evaluated and validated energy levels are called MARVEL energy levels.

In this work the steps presented below were followed to go from measured and assigned experimental transitions to MARVEL energy levels. For further details, please consult the original publications, especially refs 50 and 52.

First, all experimental data were gathered from the literature. Table 1 lists the experimental sources of transition data collected during the course of the present study (each data source is given a tag based on the year of publication and letters from the names of the author(s)). In order to be used in MARVEL, each transition has to have an initial nonzero uncertainty. Ideally, these can be taken directly from the source but in several cases they had to be guessed from the papers describing the measurements. No recalibration of the source data was attempted.

Second, a test facility was developed to check all transitions for uniqueness, including uniqueness of the label (note that all labels have been rewritten according to a redundant set of quantum numbers and symmetry information, see below), to avoid duplicating the same datum, and for consistency. Conflicts arising from the transcription of data were identified and corrected.

Third, MARVEL was executed. At this stage the uncertainties of the lines were adjusted via robust reweighting[66] until a consistent set of experimental uncertainties, within the limits of the present database, was obtained. Uncertainties of energy levels reported in this paper are given by eq 5 of ref 52 and correspond to 95% confidence limits. Due to the lack of measured microwave transitions connecting the rotational energy levels on the ground vibrational state, we were forced to use a minimum number of so-called combination difference (CD) "transitions" in order to stabilize the SN and keep the number of floating components to a minimum. Without these data several energy levels would not be determined by MARVEL. These CD transitions come from the sources 04OkEp[44] and 84WaFoMcBe,[26] containing 69 and 6 CD transitions, respectively. In the Supporting Information the CD transitions are labeled by CD.

Fourth, the MARVEL energy levels and their labels were checked against results from variational nuclear-motion computations. At this stage a few transitions yielding energy levels incompatible with clear trends observable in the deviations between variational and MARVEL energy levels (Figure 1) were removed.

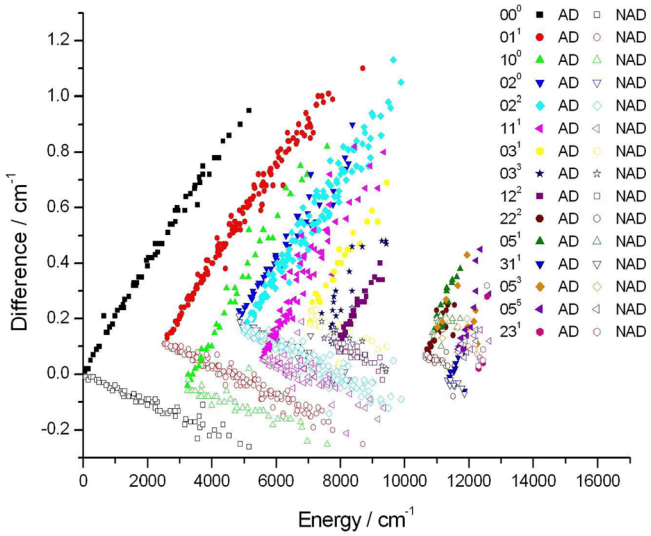

Figure 1. Deviations between MARVEL (experimental) and first-principles computed rovibrational energy levels, with AD = "adiabatic model" and NAD = "nonadiabatic model", for several vibrational bands of H_3^+. The NAD model corresponds to a computation on a single adiabatic potential energy surface with a slightly increased "vibrational" mass as compared to the nuclear "rotational" mass.

3. COMPONENTS OF THE SN OF H_3^+

The rotational−vibrational transitions characterizing one-photon (absorption or emission) experiments form a spectroscopic network (SN),[59,60] which is a large, finite, weighted, rooted graph, where the vertices are discrete energy levels (with uncertainties to be determined), the edges are transitions (with measured uncertainties), and the weights are provided by transition intensities. Components of a SN contain all interconnecting rotational−vibrational energy levels supported by the grand database of the transitions. This means, for example, that transitions involving "ortho" or "para" nuclear spin isomers of H_3^+ form separate components.

3.1. Symmetry Requirements. For H_3^+, belonging to the D_{3h}(M) molecular symmetry (MS) group,[67] the eight possible nuclear spin states span the representation $\Gamma_{ns}^{tot} = 4A_1' \oplus 2E'$ (ns = nuclear spin), providing spin-statistical weights for the rovibronic (rve) states with different Γ_{rve} symmetry labels. States with A_1' symmetry spin functions are called "ortho" states with a total nuclear spin of $I = 3/2$, while states with E' symmetry spin functions are called "para" states with $I = 1/2$ total nuclear spin. As $\Gamma_{rve} \otimes \Gamma_{ns} \supset \Gamma^+$ or $\Gamma_{rve} \otimes \Gamma_{ns} \supset \Gamma^-$ must hold, where $\Gamma^+ = A_2'$ and $\Gamma^- = A_2''$ correspond to even and odd parities, respectively, the allowed rotational−vibrational symmetries on the singlet ground electronic state are A_2' and A_2''

dx.doi.org/10.1021/ct4004355 | J. Chem. Theory Comput. 2013, 9, 5471−5478

(with a spin-statistical weight (SSW) of 4) for $\Gamma_{ns} = A_1'$, while E' and E'' for $\Gamma_{ns} = E'$ (with a spin-statistical weight of 2, counting the rotational−vibrational states of E' or E'' symmetry twice). On the basis of the work of Watson,[68] the SSWs and the symmetry properties of the rovibrational states expressed in terms of approximate quantum numbers are listed in Table 2 (the quantum numbers are explained in the next subsection).

Table 2. Symmetry Characteristics of the Observable Rovibrational States of H_3^+ within the D_{3h}(M) Molecular Symmetry Group, Based on Approximate Quantum Numbers[a]

Γ_{rve}	$G + \nu_2$	(G mod 3)	SSW
A_2'	even	= 0	4
A_2''	odd	= 0	4
E'	even	≠ 0	2
E''	odd	≠ 0	2

[a] Γ_{rve} = rovibronic symmetry species, SSW = spin statistical weight factor, while quantum numbers G and ν_2 are defined in section 3.2.

3.2. Quantum Numbers and Selection Rules. The structure of the allowed rovibrational transitions of H_3^+ is that of an oblate symmetric top. Vibrational states are described by the ν_1, ν_2, and l_2 quantum numbers, where l_2 is the vibrational angular momentum quantum number of the degenerate ν_2 mode. Rotations are described by the rigorous quantum number J and the rotational angular momentum quantum number k (and $K = |k|$) corresponding to the projection of the rotational angular momentum **J** on the C_3 symmetry axis. Neither l_2 nor k are "good" quantum numbers. It turns out that the quantum number $g = k - l_2$ is a more robust quantum number,[69] and thus, it is better to use $G = |g|$ to describe the rovibrational states of H_3^+.

Several conventions have been developed for labeling the rovibrational transitions of H_3^+ with quantum numbers. The labeling ambiguities result from the fact that spectroscopists prefer to employ approximate quantum numbers and these can be chosen with some arbitrariness, especially for a symmetric top.

In the present study we decided to employ labels with redundant information to describe rovibrational energy levels. Our label contains eight descriptors, in the order given below. The vibrational excitation is described by the three-member list ν_1 ν_2 L_2, as it is usual for this symmetric-top molecule, where $L_2 = |l_2|$. The rovibrational states are further labeled by J, G, U, K, and Γ_{rv}. Here, U denotes the U-notation of Watson,[68] also employed by Lindsay and McCall,[16] where $U = (ul|lm)$, and u means upper, l means lower, and m means that this information is unimportant. Nuclear motion computations yield J and Γ_{rv}, a symmetry descriptor, without difficulty. Some of the other descriptors can also be extracted from nuclear motion wave functions; in particular, we made a concerted effort to determine K this way (vide infra).

The selection rules related to approximate quantum numbers are based on the symmetry relations presented in Table 2.[16,67−69] Transitions are only allowed between A_2' and A_2'' states or between E' and E'' states. This can be expressed by the following rules: (G mod 3) cannot change between zero and nonzero and $\Delta(G + \nu_2)$ = odd. On the basis of the possible values of l_2, the latter selection rule can be rewritten as Δk = odd. Further selection rules are $\Delta J = 0, \pm 1$ and $\Delta k = 3$. Finally, we reiterate (see Table 2) that due to symmetry requirements, o-H_3^+ exists only with $G = 3m$, where m is an integer, and p-H_3^+ exists only with $G = 3m \pm 1$. The parity of the rotational levels is given as $(-1)^K$.

3.3. Magic Numbers. MARVEL results in the correct energy levels in an absolute sense for components not connected to the ortho or para roots only if the value of the lowest-energy level within the higher-energy component, zero by definition, is shifted to the correct transition energy. It is somewhat difficult to connect these so-called floating components to the two principal components. Due to the limited amount of pure rotation data for H_3^+, its SN contains several floating components (Table 4, vide infra).

In order to have energy levels correct in an absolute sense, two "magic numbers" are needed even if only the two principal components of the SN, ortho or para, are considered. One of the magic numbers must be introduced as the lowest vibrational state is a "missing" state, as required by the Pauli principle, and thus does not appear during the MARVEL analysis. The artificial transition, with an upper rotational label of (J K U) = (1 0 m) and with a wavenumber of 86.960(0) cm^{-1}, is thus introduced for the ortho component, taken from ref 16. The other magic number connects the lowest member of the para component to that of the ortho ground state, the rotational label of the upper state is (J K U) = (1 1 m), and the wavenumber of 64.121(0) cm^{-1} is taken also from ref 16.

4. NUCLEAR-MOTION COMPUTATIONS

The variational nuclear-motion computations, used to validate the experimental (MARVEL) transition wavenumbers, the derived energy levels, and their labels, are based on the use of a highly accurate adiabatic PES called GLH3P.[13,14] They were performed with improved versions of the in-house D^{2}FOPI[70] and GENIUSH[71,72] codes, adjusted for the purposes of the present study. Some of the computations provide exact and approximate quantum numbers and symmetry descriptions which are used to validate the experimental labels of the energy levels involved in the measured transitions. All nuclear-motion computations whose results are reported, see the Supporting Information, are converged to better than 0.01 cm^{-1} in the (ro)vibrational energies.

4.1. D^{2}FOPI Computations. The Jacobi (also known as scattering) coordinate system[73] and the R_2 embedding[74,75] were chosen to set up the rovibrational kinetic energy operator within the D^{2}FOPI code. As required by the use of an adiabatic PES, nuclear masses, m_H = 1.007 276 5 u, were employed. In the R_2 embedding the z-axis of the body-fixed frame is chosen to lie parallel to the interatomic vector described by the R_2 coordinate. Use of this coordinate system and embedding makes it possible to exploit a C_{2v}(M) symmetry of the H_3^+ molecule. Although the full symmetry of H_3^+ is D_{3h}(M), the C_{2v}(M) symmetry labels can be used to assign each rovibrational state with the appropiate D_{3h}(M) symmetry labels as well, as long as the degenerate E' and E'' symmetry states of D_{3h}(M) are computed in the two corresponding irreducible representations of C_{2v}(M) with sufficient accuracy to achieve numerical degeneracy (10^{-2} cm^{-1} was used as a threshold in this work). The A_1', A_1'', A_2', A_2'', E', and E'' irreducible representations of D_{3h}(M) are identified in the C_{2v}(M) symmetry blocks as A_1, A_2, B_2, B_1, $A_1 \oplus B_2$, and $A_2 \oplus B_1$, respectively.

To obtain the matrix representation of the chosen Hamiltonian an orthogonal, normalized, and symmetry-adapted product basis of the form $\{\chi_{n_1}(R_1)\chi_{n_2}(R_2)$

dx.doi.org/10.1021/ct4004355 | J. Chem. Theory Comput. 2013, 9, 5471−5478

$P_l^{K_z}(\cos\Theta)C_{MK_z}^{Jp}(\phi,\chi,\psi)\}_{n_1=1,n_2=1,K_z=p,l=K_z}^{N_1,N_2,J,K_z+N_L-1}$ was utilized, where R_1, R_2, and Θ are the two stretching-type and one bending-type Jacobi coordinates, respectively, $\chi_{n_1}(R_1)$ and $\chi_{n_2}(R_2)$ are DVR basis functions, $P_l^{K_z}(\cos\Theta)$ is the lth normalized associated Legendre function, $C_{MK_z}^{Jp}(\phi,\chi,\psi)$ are rotational functions of the form $C_{MK_z}^{Jp}(\phi,\chi,\psi) = (2(1+\delta_{K_{z,0}}))^{-1/2}(D_{MK_z}^{J} + (-1)^{p+K_z+J}D_{M-K_z}^{J})$, $p \in \{0, 1\}$, $K_z \in \{p, p+1, ..., J-1, J\}$ where p is a parity-like variable,[76] M and K_z are the usual quantum numbers corresponding to space- and body-fixed projections of the rotational angular momentum on the appropriate axes, and $D_{MK_z}^{J}$ are the normalized Wigner rotation functions.[76] The subsets of basis functions which transform according to the four irreducible representations of the $C_{2v}(M)$ molecular symmetry group are obtained by setting $p = 0$ or 1 and by choosing $(l + K_z)$ to be odd or even.

Due to the "almost" direct-product nature of the basis set (almost refers to the coupling between the $P_l^{K_z}(\cos\Theta)$ associated Legendre functions and the $C_{MK_z}^{Jp}(\phi,\chi,\psi)$ rotation functions via K_z and the parity of $(l + K_z)$), the matrix representation of the triatomic (ro)vibrational Hamiltonian can be written as a sum of direct-product matrices. In order to have a compact basis expansion, $\chi_{n_1}(R_1)$ and $\chi_{n_2}(R_2)$ were chosen to be potential optimized (PO) DVR functions.[77−79] The PO−DVR functions were obtained from the eigenfunctions of the 1D effective Hamiltonian $\hat{H}_J^{1D} = -((1/2\mu_j)(d^2/dR_j^2) + (L(L+1)/2\mu_j R_j^2) + \hat{V}(R_j; R_{j'}, \Theta))$, $j, j' = 1, 2$ or 2, 1 with $\hat{V}(R_j; R_{j'}, \Theta)$ chosen to be a relaxed 1D potential, i.e., $\hat{V}(R_j; R_{j'}, \Theta)$ is obtained by optimizing the $R_{j'}$ and Θ coordinates for each value of R_j. For A_1- and B_1-symmetry states, $L = 0$, while for A_2- and B_2-symmetry states, $L = 1$ was chosen to accelerate convergence. It proved to be sufficient to employ 40 basis functions along each internal coordinate to achieve the required 0.01 cm^{-1} accuracy. A variant of the Lanczos algorithm[80−82] was employed to obtain the required eigenpairs.

The rigid-rotor symmetric-top quantum label k is used in this work as an approximate quantum number, it corresponds to the projection of the angular momentum to the body-fixed axis perpendicular to the molecular plane, the y-axis in the embedding used in our nuclear motion computations. Thus, the approximate $K = |k|$ labels were computed in a given Ψ_{rovib} rovibrational state as $K = \langle\Psi_{rovib}|\hat{J}_y^2|\Psi_{rovib}\rangle^{1/2}$.

4.2. GENIUSH Computations. In order to cover some of the nonadiabatic effects,[83−85] important for this light molecular ion, different rotational and vibrational masses were employed, following the recommendations of Moss[85] and later of Polyansky and Tennyson.[9]

For the variational solution of the time-independent Schrödinger equation of the nuclei with different rotational and vibrational masses the original GENIUSH code[71,72] was extended. The approach is described here only briefly, details will be reported in a future publication.[86] To model nonadiabatic effects via the use of different rotational and vibrational masses, a composite G matrix was constructed by inverting the g matrices evaluated with either the rotational or the vibrational masses over a grid. The pure vibrational and rotational terms in the kinetic energy operator were constructed with the terms obtained with the corresponding masses, while the rovibrational subblock was built with the values obtained with the rotational mass.

In the actual computations the rotational mass for H was the nuclear mass of the proton, $m_{rot,H}$ = 1.007 276 5 u, while the vibrational mass had a slightly larger value, $m_{vib,H}$ = 1.007 537 2 u, following the recommendation of ref 85. The coordinate representation of the kinetic energy operator was defined by using two proton−proton distances and the cosine of the proton−proton−proton angle and a permutationally invariant embedding. To build the matrix representation for the Hamiltonian, a direct-product grid was used, constructed from PO−DVR[77−79] points for the stretching-like coordinates and Legendre-DVR points for the cosine of the angle coordinate. The number of grid points required to converge the presented energy levels to at least 0.01 cm^{-1} was not more than 35 and 65 for the stretching and the bending coordinates, respectively. The computed "nonadiabatic" energy levels were used to produce Figure 1 and they are also given in the Supporting Information along with the "adiabatic" D^2FOPI energies.

5. MARVEL ENERGY LEVELS

We have attempted to be as comprehensive as possible, including *all* known and assigned H_3^+ transitions in our MARVEL analysis. As a result, we have included multiple, distinct measurements of transitions as this helps to achieve higher accuracy during the energy level determinations. This makes the present study distinctly different from that of Lindsay and McCall,[16] who selected the supposedly best transition when analyzing measured data. The sources containing measured transitions are listed in Table 1. The MARVEL vibrational band origins (VBO) are provided in Table 3. The number of validated MARVEL energy levels in components of the SN of H_3^+ is given in Table 4.

With the exceptions of $3\nu_1$ ($(\nu_1\ \nu_2\ L_2)$ = (3 0 0) in the notation applied) and two $4\nu_2$ states ((0 4 0) and (0 4 2)), all vibrational bands below the barrier to linearity of H_3^+ have been studied experimentally. Above the barrier to linearity still only eight experimental vibrational band origins (VBOs) are known.

An important step in the validation of the MARVEL energy levels is to check them against the results of variational nuclear-motion computations. This step is of particular importance for levels determined by a single transition or for those levels interconnected by single transitions, known as a branch. At the same time the transitions were checked for consistency as the difference between observed and calculated levels generally shows great regularity as J varies for a given vibrational state and value of K. It is also important to point out that MARVEL cannot validate transitions (and thus energy levels) belonging to floating components (FC). Of the 1610 measured transitions collected, 78 belong to FCs. Since we could validate 1410 transitions, it means that there are 122 transitions which had to be deleted from the MARVEL analysis. These are given in the Supporting Information and are indicated there by a negative transition wavenumber. Some of the transitions removed may correspond to a correct experimental observation but an incorrect label. Nevertheless, it was decided not to keep these transitions in order to arrive at a fully validated, dependable, and self-consistent set of levels and lines. After careful relabeling, based perhaps on nuclear motion computations, the active feature of MARVEL can always be used to utilize these or any new transitions in a reanalysis of the complete set of experimental data.

There is one unusual though allowed case for H_3^+ where a rotationally excited state lies under the corresponding vibrational band origin. The (0 2 2 1 3 m 1 A_2'') rovibrational level has a smaller energy, 4994.8 cm^{-1}, than the energy of the (0 2 2) VBO at 4998.0 cm^{-1} . Note that a computed zero relative

dx.doi.org/10.1021/ct4004355 | J. Chem. Theory Comput. 2013, 9, 5471−5478

Table 3. MARVEL Vibrational Band Origins (VBO), Their Symmetries (sym), MARVEL Uncertainties (unc), and the Number of Rotational Levels (RL) the Vibrational Levels Are Holding within the Present Database, for H_3^+ [a]

v_1 v_2 L_2	sym	VBO/cm^{-1}	unc	RL
0 0 0	A_1'	0.0000[b]	0	63
0 1 1	E'	2521.4083	20	134
1 0 0	A_1'	c		36
0 2 0	A_1'	c		43
0 2 2	E'	4998.0479	100	118
1 1 1	E'	5554.0610	100	65
2 0 0	A_1'	c		1
0 3 1	E'			23
0 3 3	A_2'	7492.9112	50	18
1 2 0	A_1'	c		6
1 2 2	E'			32
2 1 1	E'			2
0 4 4	E'			3
2 2 0	A_1'	c		1
2 2 2	E'	10645.3770	100	22
0 5 1	E'	10862.9007	33	17
3 1 1	E'	11323.0960	100	12
0 5 3	A_2'			10
0 5 5	E'	11658.3970	100	14
1 4 0	A_1'	c		4
1 4 2	E'			5
2 3 1	E'	12303.3630	100	6
0 6 2	E'	12477.3780	100	4
2 3 3	A_1'	c		1
1 4 4	E'			4
3 2 2	E'			1
0 7 1	E'	13702.3720	50	1
1 6 2	E'			2
0 8 2	E'	15122.8010	50	1
1 6 4	E'			1
2 5 1	E'			1
3 4 2	E'			1

[a]The uncertainties (unc) are given in units of 10^{-4} cm^{-1} . The VBOs are ordered according to their energies. [b]The value of the vibrational ground state was fixed to zero with zero uncertainty. Note that, due to its symmetry, this is a "missing" state (see text). [c]Due to its symmetry, this is a "missing" VBO (see text).

Table 4. Summary of the MARVEL Energy Levels Determined for H_3^+ during the Present Study

component	number
o-H_3^+	259
p-H_3^+	393
FC[a]	105
sum	757

[a]FC = floating component of the spectroscopic network (see text). Number of transitions forming FCs is 74. These transitions and energy levels cannot be validated via MARVEL though they may be correct.

energy of rovibrational states compared to the vibrational state was documented recently for the CH_4F^- complex.[87]

It is worth mentioning that the transitions formed by the MARVEL energy levels reproduce the 12 highly accurate transitions measured by Shy et al.,[49] which have a claimed accuracy of about 0.0004 cm^{-1}, with an average accuracy of 0.0001 cm^{-1}. This nice agreement increases our confidence in many of the other MARVEL energy levels, as well.

6. NONADIABATIC CORRECTIONS

In 2006, Alijah and Hinze[88] provided a thorough analysis of the nonadiabatic effect for the rovibrational levels of H_3^+ based on some simple linear and quadratic correction functions. Their study was hindered by the fact that no rovibrational energies higher than about 10 000 cm^{-1}, close to the barrier to linearity, were available to them. On the basis of the availability of MARVEL energy levels up to 16 500 cm^{-1}, it is time to reconsider nonadiabatic corrections for this molecule.

Figure 1 plots the difference between our MARVEL energy level data set and the corresponding levels computed variationally either within the adiabatic (AD) or nonadiabatic (NAD) approximation. The exceptional quality of the GLH3P adiabatic PES[13,14] can be seen from the small differences between the adiabatic and MARVEL energy levels. The substantial difference between the two sets of first-principles results, the systematic nature of the nonadiabatic effect for each vibrational band, and the overall improvement provided by the increased vibrational mass of H is clearly visible in Figure 1. These results should prove to be useful for future more extended studies of the nonadiabatic effect, perhaps based on the concept of coordinate-dependent mass surfaces (CDMS).[11,83,84]

7. SUMMARY AND CONCLUSIONS

Among the species for which spectroscopic data are needed for important scientific applications concerning, for example, the interstellar medium, the isotopologues of H_3^+ are of central importance. Thus, the study of their spectra is of prime interest. At the same time, this task provides a fertile testing ground for different experimental and theoretical approaches yielding the required information.

It would be convenient if high-resolution molecular spectroscopy experiments could yield the required line-by-line information. However, while experiments yield accurate and often precise data, the amount of information that can be obtained is only a small fraction of that required. Quantum theory, on the other hand, can result in the full information,[51,89] but the accuracy of even the most sophisticated treatments[13] is considerably worse, especially for line positions, than that of experiments. Therefore, the best possible approach one can take is to use all the available experimental and quantum mechanical information to come up with a linelist as accurate as allowed by the available data. This study, employing the MARVEL algorithm to validate transitions and obtain experimental quality rovibrational energy levels for H_3^+, is a contribution toward this goal. As proven in this work, the MARVEL approach,[50−53] combined with results from variational nuclear motion computations, provides an ideal platform to achieve the goal of determining accurate rovibrational energy levels from which a lot of accurate line positions can be calculated straightforwardly.

Accuracy of the energy levels determined in this study is dependent upon several factors. Most important among these is the accuracy of the observed transitions. Since our analysis utilized all available experimental information, there are many energy levels which are involved in multiple transitions measured by different experimental groups utilizing different spectrometers and experimental conditions and forming cycles (closed walks) within the spectroscopic network, ensuring the improved accuracy of the MARVEL energy levels.

The present study also suggests that determination of an accurate set of energy levels requires not only dependable experimental data but also a first-principles approach to determine as accurate energy levels as possible. This was provided here by variational nuclear motion computations employing the most accurate adiabatic PES of H_3^+, called GLH3P.[13,14] While the adiabatic GLH3P PES has an intrinsic estimated accuracy of a few 0.01 cm^{-1} with respect to the exact Born−Oppenheimer PES, converged rovibrational energy levels computed with it variationally using an exact kinetic energy operator are much less accurate, deviations up to 1 cm^{-1} are observed for higher excitations. These deviations are due to what one may call nonadiabatic effects. Using a slightly increased value for the vibrational mass, following the work of Moss[85] and Polyansky and Tennyson,[9] results in an improved agreement with experiment. For further improvement, one needs a more sophisticated treatment, perhaps the one provided by coordinate-dependent masses[11,83,84,90,91] or the one following the scheme developed by Schwenke[92] and employed successfully for water.[93]

■ ASSOCIATED CONTENT

Supporting Information

MARVEL input file with measured transitions; MARVEL output file with refined energy levels; tables containing MARVEL energy levels along with their variationally computed counterparts used to generate Figure 1, separated for each vibrational band; a ReadMe.txt file explaining the headings of the various files. This material is available free of charge via the Internet at http://pubs.acs.org.

■ AUTHOR INFORMATION

Corresponding Author

*E-mail: csaszar@chem.elte.hu.

Notes

The authors declare no competing financial interest.

■ ACKNOWLEDGMENTS

The authors would like to thank the Scientific Research Fund of Hungary (grant OTKA NK83583) for support of the research described. The authors are grateful to Mr. Amir Bagheri Garmarudi and Mr. István Szabó for their help with data processing at an early stage of the project. EM thanks the NIIF Institute for providing access to the computing facilities in Debrecen, Hungary.

■ REFERENCES

(1) McCall, B. J.; Oka, T. *Science* **2000**, *287*, 1941−1942.
(2) Oka, T. *Rev. Mod. Phys.* **1992**, *45*, 1141−1149.
(3) Tennyson, J. *Rep. Prog. Phys.* **1995**, *57*, 421−476.
(4) Krogh, H. *Phil. Trans. R. Soc. A* **2012**, *370*, 5225−5235.
(5) Herbst, E.; Klemperer, W. *Astrophys. J.* **1973**, *185*, 505−533.
(6) Herbst, E. *Phil. Trans. R. Soc. Lond. A* **2000**, *358*, 2523−2534.
(7) Miller, S.; Stallard, T.; Melin, H.; Tennyson, J. *Faraday Discuss.* **2010**, *147*, 283−291.
(8) Polyansky, O. L.; Alijah, A.; Zobov, N. F.; Mizus, I. I.; Ovsyannikov, R. I.; Tennyson, J.; Lodi, L.; Szidarovszky, T.; Császár, A. G. *Phil. Trans. R. Soc. A* **2012**, *370*, 5014−5027.
(9) Polyansky, O. L.; Tennyson, J. *J. Chem. Phys.* **1999**, *110*, 5056−5064.
(10) Jaquet, R.; Carrington, T. *J. Phys. Chem. A* **2013**, *117*, 9493−9500.
(11) Diniz, L. G.; Mohallem, J. R.; Alijah, A.; Pavanello, M.; Adamowicz, L.; Polyansky, O. L.; Tennyson, J. *Phys. Rev. A* **2013**, *88*, 032506.
(12) Friedrich, O.; Alijah, A.; Xu, Z.; Varandas, A. J. C. *Phys. Rev. Lett.* **2001**, *86*, 1183−1186.
(13) Pavanello, M.; Adamowicz, L.; Alijah, A.; Zobov, N. F.; Mizus, I. I.; Polyansky, O. L.; Tennyson, J.; Szidarovszky, T.; Császár, A. G.; Berg, M.; Petrignani, A.; Wolf, A. *Phys. Rev. Lett.* **2012**, *108*, 023001.
(14) Pavanello, M.; Adamowicz, L.; Alijah, A.; Zobov, N. F.; Mizus, I. I.; Polyansky, O. L.; Tennyson, J.; Szidarovszky, T.; Császár, A. G. *J. Chem. Phys.* **2012**, *136*, 184303.
(15) Oka, T. *Phys. Rev. Lett.* **1980**, *45*, 531−534.
(16) Lindsay, C. M.; McCall, B. J. *J. Mol. Spectrosc.* **2001**, *210*, 60−83.
(17) Polyansky, O. L.; Dinelli, B. M.; Le Sueur, C. R.; Tennyson, J. *J. Chem. Phys.* **1995**, *102*, 9322−9326.
(18) Bramley, M. J.; Tromp, J. W.; Carrington, T., Jr.; Corey, G. C. *J. Chem. Phys.* **1994**, *100*, 6175−6194.
(19) Mandelshtam, V A; Taylor, H S *J. Chem. Phys.* **1997**, *106*, 5085−5090.
(20) Jensen, P.; Paidarova, I.; Spirko, V.; Sauer, S. P. A. *Mol. Phys.* **1997**, *91*, 319−332.
(21) Kostin, M. A.; Polyansky, O. L.; Tennyson, J.; Mussa, H. Y. *J. Chem. Phys.* **2003**, *118*, 3538−3542.
(22) Silva, B. C.; Barletta, P.; Munro, J. J.; Tennyson, J. *J. Chem. Phys.* **2008**, *128*, 244312.
(23) Szidarovszky, T.; Császár, A. G.; Czakó, G. *Phys. Chem. Chem. Phys.* **2010**, *12*, 8373−8386.
(24) Oka, T. *Phil. Trans. R. Soc. Lond. A* **1981**, *303*, 543−549.
(25) Morong, C. P.; Gottfried, J. L.; Oka, T. *J. Mol. Spectrosc.* **2009**, *255*, 13−23.
(26) Watson, J. K. G.; Foster, S. C.; McKellar, A. R. W.; Bernath, P.; Amano, T.; Pan, F. S.; Crofton, M. W.; Altman, R. S.; Oka, T. *Can. J. Phys.* **1984**, *62*, 1875−1885.
(27) Majewski, W. A.; Marshall, M. D.; McKellar, A. R. W.; Johns, J. W. C.; Watson, J. K. G. *J. Mol. Spectrosc.* **1987**, *62*, 341−355.
(28) Majewski, W. A.; Feldman, P. A.; Watson, J. K. G.; Miller, S.; Tennyson, J. *Astrophys. J.* **1989**, *347*, LS1−L54.
(29) Nakanaga, T.; Ito, F.; Sugawara, K.; Takeo, H.; Matsumura, C. *Chem. Phys. Lett.* **1990**, *169*, 269−273.
(30) Bawendi, M. G.; Rehfuss, B. D.; Oka, T. *Chem. Phys. Lett.* **1990**, *93*, 6200−6209.
(31) Xu, L.-W.; Gabrys, C.; Oka, T. *J. Chem. Phys.* **1990**, *93*, 6210−6215.
(32) Lee, S. S.; Ventrudo, B. F.; Cassidy, D. T.; Oka, T.; Miller, S.; Tennyson, J. *J. Mol. Spectrosc.* **1991**, *145*, 222−224.
(33) Kao, L.; Oka, T.; Miller, S.; Tennyson, J. *Astrophys. J.* **1991**, *77*, 317−329.
(34) Xu, L.-W.; Rosslein, M.; Gabrys, C. M.; Oka, T. *J. Mol. Spectrosc.* **1992**, *153*, 726−737.
(35) Ventrudo, B. F.; Cassidy, D. T.; Guo, Z. Y.; Joo, S.; Lee, S. S.; Oka, T. *J. Chem. Phys.* **1994**, *100*, 6263−6266.
(36) Uy, D.; Gabrys, M.; Jagod, M.-F.; Oka, T. *J. Chem. Phys.* **1994**, *100*, 6267−6274.
(37) Majewski, W. A.; McKellar, A. R. W.; Sadovskii, D.; Watson, J. K. G. *Can. J. Phys.* **1994**, *72*, 1016−1027.
(38) McKellar, A. R. W.; Watson, J. K. G. *J. Mol. Spectrosc.* **1998**, *191*, 215−217.
(39) Joo, S.; Kuhnemann, F.; Jagod, M.-F.; Oka, T. Diode Laser Observation of the High J P(12,12)+ Transition of H_3^+. *Poster Presented at The Royal Society Discussion Meeting on Astronomy, Physics and Chemistry of* H_3^+; London, Feb 9−10, 2000
(40) McCall, B. J.; Oka, T. *J. Mol. Spectrosc.* **2000**, *113*, 3104−3110.
(41) McCall, B. J. *Phil Trans. R. Soc. London A* **2001**, *358*, 2385−2401.
(42) Lindsay, C. M.; Rade, R. M., Jr.; Oka, T. *J. Mol. Spectrosc.* **2001**, *210*, 51−59.
(43) Gottfried, J. L.; McCall, B. J.; Oka, T. *J. Chem. Phys.* **2003**, *118*, 1−10.
(44) Oka, T.; Epp, E. *Astrophys. J.* **2004**, *613*, 349−354.

(45) Mikosch, J.; Kreckel, H.; Wester, R.; Plasil, R.; Glosik, J.; Gerlich, D.; Schwalm, D.; Wolf, A. *J. Chem. Phys.* **2004**, *121*, 11030−11037.
(46) Gottfried, J. L. *Phil. Trans. R. Soc. A* **2006**, *364*, 2917−2929.
(47) Kreckel, H.; Bing, D.; Reinhardt, S.; Petrignani, A.; Berg, M.; Wolf, A. *J. Chem. Phys.* **2008**, *129*, 164312.
(48) Crabtree, K. N.; Hodges, J. N.; Siller, B. M.; Perry, A. J.; Kelly, J. E.; Jenkins, P. A.; McCall, B. J. *Chem. Phys. Lett.* **2012**, *551*, 1−6.
(49) Wu, K.-Y.; Liena, Y.-H.; Liao, C.-C.; Lin, Y.-R.; Shy, J.-T. *Phys. Rev. A* **2013**, *88*, 032507.
(50) Furtenbacher, T.; Császár, A. G. *J. Quant. Spectrosc. Radiat. Transfer* **2012**, *113*, 929−935.
(51) Császár, A. G.; Czakó, G.; Furtenbacher, T.; Mátyus, E. *Ann. Rep. Comp. Chem.* **2007**, *3*, 155−176.
(52) Furtenbacher, T.; Császár, A.; Tennyson, J. *J. Mol. Spectrosc.* **2007**, *245*, 115−125.
(53) Furtenbacher, T.; Császár, A. G. *J. Quant. Spectr. Rad. Transfer* **2008**, *109*, 1234−1251.
(54) Tennyson, J.; Bernath, P. F.; Brown, L. R.; Campargue, A.; Carleer, M. R.; Császár, A. G.; Gamache, R. R.; Hodges, J. T.; Jenouvrier, A.; Naumenko, O. V.; Polyansky, O. L.; Rothman, L. S.; Toth, R. A.; Vandaele, A. C.; Zobov, N. F.; et al. *J. Quant. Spectrosc. Radiat. Transfer* **2009**, *110*, 573−596.
(55) Tennyson, J.; Bernath, P. F.; Brown, L. R.; Campargue, A.; Császár, A. G.; Daumont, L.; Gamache, R. R.; Hodges, J. T.; Naumenko, O. V.; Polyansky, O. L.; Rothman, L. S.; Toth, R. A.; Vandaele, A. C.; Zobov, N. F.; Fally, S.; et al. *J. Quant. Spectrosc. Radiat. Transfer* **2010**, *111*, 2160−2184.
(56) Tennyson, J.; Bernath, P. F.; Brown, L. R.; Campargue, A.; Császár, A. G.; Daumont, L.; Gamache, R. R.; Hodges, J. T.; Naumenko, O. V.; Polyansky, O. L.; Rothman, L. S.; Van-daele, A. C.; Zobov, N. F.; Al Derzi, A. R.; Fábri, C.; et al. *J. Quant. Spectrosc. Radiat. Transfer* **2013**, *117*, 29−80.
(57) Fábri, C.; Mátyus, E.; Furtenbacher, T.; Nemes, L.; Mihaly, B.; Zoltáni, T.; Császár, A. G. *J. Chem. Phys.* **2011**, *135*, 094307.
(58) Furtenbacher, T.; Szidarovszky, T.; Fábri, C.; Császár, A. G. *Phys. Chem. Chem. Phys.* **2013**, *15*, 10181−10193.
(59) Császár, A. G.; Furtenbacher, T. *J. Mol. Spectrosc.* **2011**, *266*, 99−103.
(60) Furtenbacher, T.; Császár, A. G. *J. Mol. Struct.* **2012**, *1009*, 123−129.
(61) Neale, L.; Miller, S.; Tennyson, J. *Astrophys. J.* **1996**, *464*, 516−520.
(62) Carrington, A.; Buttenshaw, J.; Kennedy, R. A. *Mol. Phys.* **1982**, *45*, 753−758.
(63) Carrington, A.; Kennedy, R. A. *J. Chem. Phys.* **1984**, *81*, 91−112.
(64) Dinelli, B. M.; Neale, L.; Polyansky, O. L.; Tennyson, J. *J. Mol. Spectrosc.* **1997**, *181*, 142−150.
(65) Velilla, L.; Lepetit, B.; Aguado, A.; Beswick, J. A.; Paniagua, M. *J. Chem. Phys.* **2008**, *129*, 084307.
(66) Watson, J. K. G. *J. Mol. Spectrosc.* **2003**, *219*, 326−328.
(67) Bunker, P. R.; Jensen, P. *Molecular Symmetry and Spectroscopy*; NRC Research Press: Ottawa, 1998.
(68) Watson, J. K. G. *J. Mol. Spectrosc.* **1984**, *103*, 350−363.
(69) Hougen, J. T. *J. Chem. Phys.* **1962**, *37*, 1433−1441.
(70) Szidarovszky, T.; Fábri, C.; Császár, A. G. *J. Chem. Phys.* **2012**, *136*, 174112.
(71) Mátyus, E.; Czakó, G.; Császár, A. G. *J. Chem. Phys.* **2009**, *130*, 134112.
(72) Fábri, C.; Mátyus, E.; Császár, A. G. *J. Chem. Phys.* **2011**, *134*, 074105.
(73) Jacobi, C. G. J. *Cr. Hebd. Acad. Sci.* **1842**, *15*, 236.
(74) Sutcliffe, B. T.; Tennyson, J. *Int. J. Quantum Chem.* **1991**, *39*, 183−196.
(75) Tennyson, J.; Sutcliffe, B. T. *J. Chem. Phys.* **1982**, *77*, 4061−4072.
(76) Zare, R. N. *Angular Momentum: Understanding Spatial Aspects in Chemistry and Physics*; Wiley-Interscience: New York, 1988.
(77) Wei, H.; Carrington, T., Jr. *J. Chem. Phys.* **1992**, *97*, 3029−3037.
(78) Echave, J.; Clary, D. C. *Chem. Phys. Lett.* **1992**, *190*, 225−230.
(79) Szalay, V.; Czakó, G.; Nagy, A.; Furtenbacher, T.; Császár, A. G. *J. Chem. Phys.* **2003**, *119*, 10512−10518.
(80) Lanczos, C. *J. Res. Natl. Bur. Stand.* **1950**, *45*, 255.
(81) Cullum, J. K.; Willoughby, R. A. *Lanczos Algorithms for Large Symmetric Eigenvalue Computations*; Birkhauser: Boston, 1985.
(82) Saad, Y. *Iterative Methods for Sparse Linear Systems*; Society for Industrial and Applied Mathematics: Philadelphia, PA, 2003.
(83) Bunker, P. R.; Moss, R. E. *Mol. Phys.* **1977**, *33*, 417−424.
(84) Bunker, P. R.; Moss, R. E. *J. Mol. Spectrosc.* **1980**, *80*, 217−228.
(85) Moss, R. E. *Mol. Phys.* **1996**, *89*, 195−210.
(86) Mátyus, E.; Császár, A. G. to be published.
(87) Fábri, C.; Császár, A. G.; Czakó, G. *J. Phys. Chem. A* **2013**, *117*, 6975−6983.
(88) Alijah, A.; Hinze, J. *Phil. Trans. R. Soc. A* **2006**, *364*, 2877−2888.
(89) Császár, A. G.; Fábri, C.; Szidarovszky, T.; Mátyus, E.; Furtenbacher, T.; Czakó, G. *Phys. Chem. Chem. Phys.* **2012**, *14*, 1085−1106.
(90) Kutzelnigg, W. *Mol. Phys.* **2007**, *105*, 2627−2647.
(91) Pachucki, K.; Komasa, J. *J. Chem. Phys.* **2009**, *130*, 164113.
(92) Schwenke, D. W. *J. Phys. Chem. A* **2001**, *105*, 2352−2360.
(93) Polyansky, O. L.; Császár, A. G.; Shirin, S. V.; Zobov, N. F.; Barletta, P.; Tennyson, J.; Schwenke, D. W.; Knowles, P. J. *Science* **2003**, *299*, 539−542.